A LETTERS JOURNAL EXPLORING THE FRONTIERS OF PHYSICS

OFFPRINT

Quantification of droplet deformation by electromagnetic trapping

P. C. F. Møller and L. B. Oddershede

EPL, **88** (2009) 48005

A Letters Journal Exploring the Frontiers of Physics

November 2009

EPL, **88** (2009) 48005
doi: 10.1209/0295-5075/88/48005

www.epljournal.org

Quantification of droplet deformation by electromagnetic trapping

P. C. F. Møller and L. B. Oddershede[(a)]

Niels Bohr Institute, University of Copenhagen - Blegdamsvej 17, 2100 Copenhagen, Denmark, EU

received 18 September 2009; accepted in final form 6 November 2009
published online 3 December 2009

PACS 87.80.Cc – Optical trapping
PACS 42.50.Wk – Mechanical effects of light on material media, microstructures and particles

Abstract – A tightly focused laser beam exerting a trapping force on an object also exerts deformation forces on the object. If the object is relatively easy to deform, as is, *e.g.*, a low surface tension droplet, the resulting deformation is easily detectable even at moderate laser powers. The observed deformation is analytically explained by a model, which quantitatively predicts the deformation of any micron-sized drop where the only restoring force is the surface tension. Theoretical tools are also provided to include the effect of elasticity of the shell and bulk of the trapped object, this being particularly important for deformations of cells. This deformation effect of electromagnetic radiation is important to consider while trapping soft materials and it can be used to determine physical characteristics of soft materials.

Introduction. – By tightly focusing a single laser beam an optical trap can be created. Optical traps are widely used to manipulate micro-meter–sized objects such as living cells and polystyrene beads [1] and even nano-meter–sized metallic particles are easily manipulated [2,3]. Optical traps can also be used as force-measuring tools and have proven very successful in measuring corresponding values of forces and distances in single molecule assays, where the system of interest is conjugated to a bead, which serves as a handle for the optical routines [4]. It is a well-known physical fact that one cannot perform a measurement without influencing the measured system. This principle becomes more relevant as the size of the system decreases and is of outermost significance for quantum mechanics. For micro- and macroscopic systems this effect is often not relevant in practise, however, the effect is still there and it can even be advantageously utilized for instance as shown in this letter.

Optical traps exert considerable forces on a trapped object. If the trapped material is deformable, the gradient in the light intensity will cause forces which tend to deform the object. This effect is beneficially utilized, *e.g.*, in "optical stretcher" assays [5], which are typically used to deform living cells, and where the extend of deformation gives information about the viscoelastic properties of the deformed material. The light field from an optical trap has also been used to deform biological objects such as red blood cells [6,7] from their original biconcave disk shape into a more rod-like shape, interestingly, the optically induced deformation was shown to be dependent on the physiological state of the cell. Optically held beads have been used to stretch various types of cells [8] with the goal of elucidating chemomecanical pathways. Also, multiple optical traps have been used to perform optical sculpturing of emulsion droplets [9]. However, in order to truly take the effect into consideration in measurements involving tightly focused lasers, or to take advantage of it to study physical properties of soft materials, it is important to quantify and theoretically understand the effect.

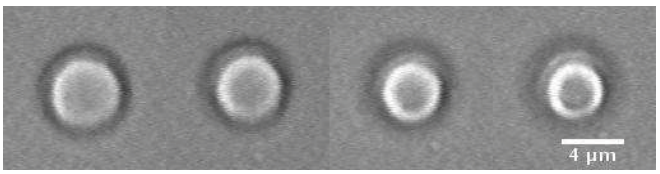

Fig. 1: Images of a low surface tension drop at different laser powers. From left to right: 40 mW, 80 mW, 126 mW, and 252 mW.

In this letter we use an optical trap based on a single infrared laser beam to deform low surface tension droplets. We show that an increase in laser power from zero to 200 mW at the sample linearly decreases the droplet diameter by as much as 20% (as shown in fig. 1) and increases the droplet length along the direction of the propagating laser light by more than 50%. Our analytical model utilizes the surface tension, the indices of

[(a)] E-mail: oddershede@nbi.dk

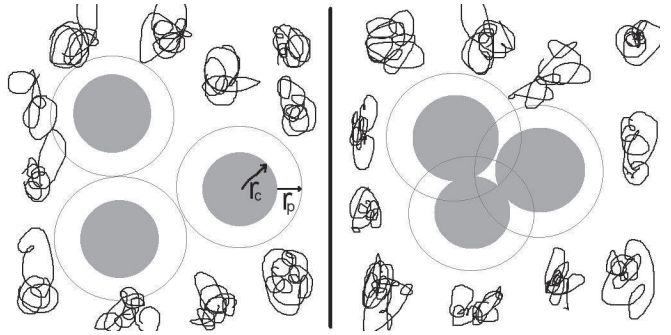

Fig. 2: Around each colloid there is a shell of thickness r_p where the polymer ball centers cannot enter (left). More space is available to the polymers when the colloids are pushed together so that the shells overlap (right). This is entropically favorable at high polymer concentrations.

refraction, and the laser power as parameters and based on these it precisely predicts the experimentally observed deformation of a droplet where the only restoring force is surface tension. We also develop analytical expressions to predict laser induced deformation of objects, such as cells, of which the restoring force arises from surface and/or bulk elasticity.

Methods. – The optical trap was implemented in an inverted Leica DMI6000 microscope, where the laser (Spectra Physics Nd:YVO_4, $\lambda = 1064\,\mathrm{nm}$, TEM_{00}) was tightly focused by a water immersion objective (Leica HCX PL APO 63×, NA 1.2) in order to minimize spherical aberrations and have a large working distance. For details on the equipment see, *e.g.*, ref. [3].

The low surface tension fluid used for the experiments was an aqueous mixture of charge-stabilized colloidal silica beads with average radius $r_c = 13\,\mathrm{nm}$ (LUDOX TM-40, from Sigma-Aldrich) [10], and cellulose polymer chains (Carboxymethyl cellulose, sodium salt, $M_W = 90000$, from Sigma-Aldrich) with a radius of gyration of approximately $r_p = 7\,\mathrm{nm}$ in water. At low polymer concentrations a homogeneous mixture results, but at higher concentrations the colloids are pushed together entropically. This is because of the excluded volume effect: Around each colloid there is a shell of a r_p thickness where the center of the polymer balls cannot enter (fig. 2). With V_{tot} being the total volume, and N_c the number of colloids, the volume available for distributing the polymer centers is: $V_{tot} - N_c 4\pi(r_c + r_p)^3/3$ if the colloids are homogeneously distributed, but about $V_{tot} - N_c 4\pi(r_c)^3/3$ if the colloids are concentrated in one phase (the liquid phase) and the polymers are concentrated in the other (the gas phase) [11]. This means that at high polymer concentrations a phase separation into a liquid and a gas phase is preferred to a homogeneous distribution.

The mixture used here consisted of water, polymer and LUDOX TM 40 in the mass fractions 0.47, 0.01, and 0.52, respectively. First, the polymer powder was dissolved in water for about 24 hours under gentle stirring. Then the dissolved polymer was slowly added to the colloids during stirring. This resulted in a fluid with roughly 25% liquid phase and 75% gas phase. The densities of the gas and liquid phases were $\rho_{gas} = 1.100\,\mathrm{g/cm^3}$ and $\rho_{liq} = 1.306\,\mathrm{g/cm^3}$, respectively. The surface tension was computed from measuring the capillary rise in glass tubes of $40 \pm 10\,\mu\mathrm{m}$ inner diameter: $\gamma = \frac{H\Delta\rho g R}{2\cos(\theta)}$, where H is the capillary rise, g the gravitational acceleration, R is the radius of the tubes, and θ is the contact angle of the liquid phase on glass [12]. Using the capillary rise in several different capillaries and setting $\theta = 0$, the surface tension was determined to be $\gamma = 1.9 \pm 0.3\,\mu\mathrm{N/m}$. The indices of refraction were measured by filling a quadratic prism cell with the materials and measuring the refraction of the laser beam. At a wavelength of 1064 nm the indices of refraction of water, the gas phase, and the liquid phase were measured to be 1.322, 1.330, and 1.366, respectively. This system has some advantages compared to other low surface tension systems previously used for deforming interfaces with light [9,13,14]; it is non-toxic, has effectively no temperature dependence (so potential laser heating is not a problem), requires no surfactants, and since it contains no organic solvents it can be stored and treated without the need for specialized containers and cells. It also has some disadvantages; a drop can grow in size with time, the temperature independence means that the sample properties cannot be altered by changing its temperature, and since it is non-toxic, also to bacteria, one has to be careful to avoid contamination.

Analytical model. –

Deformed viscous droplet dominated by surface tension. The drop is trapped in the focal point of the laser because a state where more liquid with the higher index of refraction is in the illuminated region is energetically preferable. For the same reason a drop caught at the focal point is being stretched along the laser axis, but this elongation increases the surface area, and hence the surface energy. The equilibrium deformation is then where the optical stretching force, F_{opt}, is balanced by the restoring surface tension force, F_{st}. For small deformations we approximate the drop by a prolate spheroid ($x^2/a^2 + y^2/a^2 + z^2/b^2 = 1$), where a is the horizontal, transverse radius at the equator, and b is the vertical, conjugate radius, a schematic drawing is shown in fig. 3(B). Because of volume conservation, $4\pi a^2 b/3 = 4\pi r_0^3/3 \Rightarrow a = (r_0^3/b)^{1/2}$, where r_0 is the radius of the unperturbed drop, so that $b \equiv r_0 + \Delta b \Rightarrow a = r_0 - \Delta b/2$. Consider, first, the hydrodynamic restoration force when the sphere is stretched into a spheroid. Along the equator, the total force on one half of the drop is

$$F_{st} = -2\pi a\gamma + \pi a^2 \Delta p, \tag{1}$$

where a is the equatorial radius, γ the liquid surface tension, and Δp the Laplace pressure difference between the inside and outside of the drop. The first term is the surface tension pulling the two halves together along the equator, and the second term arises from the surplus

pressure inside the drop pushing the two halves apart. Since the Laplace pressure is given by $\Delta p = \gamma(1/r_1 + 1/r_2)$, where r_1 and r_2 are the two principal radii of curvature [12] one obtains:

$$F_{st} = -2\pi a\gamma + \pi a^2\gamma(1/a + 1/b'), \tag{2}$$

where b' is the second principal radius of curvature along the equator. The Gaussian curvature along the equator of a prolate spheroid is given by

$$\frac{1}{ab'} \equiv K = \frac{1}{b^2} \Rightarrow \frac{1}{b'} = \frac{a}{b^2}, \tag{3}$$

so that

$$F_{st} = -2\pi a\gamma + \pi a^2\gamma(\frac{1}{a} + \frac{a}{b^2}) = \pi\gamma\left[-a + \frac{a^3}{b^2}\right]. \tag{4}$$

Inserting the expressions for a and b, and linearizing in Δb gives:

$$F_{st} \approx -3\pi\gamma\Delta b. \tag{5}$$

Not surprisingly, the surface tension tries to restore the spherical shape with a force proportional to the deformation, Δb.

Consider now the radiation pressure on the drop. In the small region near the laser axis where the field is significant, the drop is essentially flat, and the laser field is approximately a plane, monochromatic wave. The force on an interface is equal to the incoming momentum per unit time plus the reflected, minus the transmitted. The momentum per unit time of a light beam is given by $P/(c/n)$ where P is the laser power, c is the speed of light in vacuum, and n is the index of refraction. The optical force on the two faces of the drop is then given by [5,15]:

$$F_{opt} = \frac{n_g P}{c} Q, \tag{6}$$

$$Q_{front} = 1 + R - n(1 - R), \tag{7}$$

$$Q_{back} = (1 - R)\left[n + Rn - (1 - R)\right], \tag{8}$$

$$R = \frac{(n_g - n_l)^2}{(n_g + n_l)^2}, \quad n = n_l/n_g, \tag{9}$$

where R is the reflection coefficient and n_l and n_g are the indices of refraction for the liquid and gas phase, respectively. Inserting constants, and the measured valued for n_l and n_g gives: $F_{front} \approx -1.185 \cdot 10^{-10}\,\mathrm{s/m} \cdot P$, $F_{back} \approx 1.217 \cdot 10^{-10}\,\mathrm{s/m} \cdot P$. As expected, the optical force tries to stretch the drop along the laser direction, and there is a small net force pushing the drop along the propagation direction of the laser. This net pushing force is known as the scattering force, and it is balanced by the refraction of laser rays not parallel to the laser axis, known as the gradient force of the optical tweezers. Hence, the average stretching force is

$$F_{opt} = \frac{n_g P}{c}\langle|Q|\rangle. \tag{10}$$

By setting the total force to zero the equilibrium deformation can be found:

$$F_{opt} + F_{st} = 0 \Rightarrow \Delta b = \frac{n_g\langle|Q|\rangle}{3\pi\gamma c} P, \tag{11}$$

and since $\Delta a = -\frac{1}{2}\Delta b$ the slope of the radius *vs.* laser power is finally given by

$$\frac{\Delta a}{P} = -\frac{n_g\langle|Q|\rangle}{6\pi\gamma c} \approx -3.33\,\mu\mathrm{m/W}. \tag{12}$$

Deformed object dominated by shell elasticity. In contrast to a viscous drop, the mechanics of cells is not dominated by surface tension, but by either shell elasticity (stemming from the cell wall or membrane), bulk elasticity (from the cytoskeleton), or possibly both. We first treat the case where the cell has an elastic shell, but no bulk elasticity (*e.g.*, a procaryotic cell without a polymerized cytoskeleton). While surface tension always tries to minimize the surface area, shell elasticity tries to restore the equilibrium shape of the cell. As an example, consider a sphere where half the volume is sucked out; under such circumstances a liquid drop would simply shrink in size, but a drop with an elastic shell would buckle like a deflated basket ball or a red blood cell. This also demonstrates that for an elastic shell, buckling is cheap in terms of potential energy compared to stretching or shrinking of the surface area. Hence, the potential energy of a slightly deformed elastic shell, the buckling energy, is neglectable compared to the stretching energy. The potential energy per unit volume of a stretched elastic material is given by

$$\frac{Y}{2}\left(\frac{\Delta L}{L_0}\right)^2, \tag{13}$$

where Y is Young's modulus, L_0 the equilibrium length, and ΔL the length increase. As a first order approximation, the potential energy of a slightly deformed elastic shell is proportional to the relative area change of the surface. We assume again that the shell remains ellipsoidal for small deformations. The surface area is then given by

$$S = 2\pi\left(a^2 + b^2\frac{\theta}{\tan\theta}\right), \quad \theta = \arccos\left(\frac{a}{b}\right) \tag{14}$$

but for small deformations $a \approx b$, so $\theta \approx 0$ and $\frac{\theta}{\tan\theta} \approx 1$, so that

$$S \approx 2\pi\left(\left(r_0 - \frac{\Delta b}{2}\right)^2 + (r_0 + \Delta b)^2\right), \tag{15}$$

where r_0 and Δb is given as above. Hence, to first order we have

$$S \approx 2\pi\left(2r_0^2 + r_0\Delta b\right) \equiv S_0 + 2\pi r_0\Delta b. \tag{16}$$

Defining

$$\frac{S_0 + 2\pi r_0\Delta b}{S_0} \equiv \left(\frac{L_0 + \Delta L}{L_0}\right)^2 \tag{17}$$

and linearizing, we get

$$\frac{\Delta L}{L_0} \approx \frac{2\pi r_0 \Delta b}{4\pi r_0^2}, \tag{18}$$

so that the potential energy per unit volume is given by

$$\frac{U_{elastic}}{\text{unit volume}} \approx \frac{Y}{2}\left(\frac{\Delta b}{2r_0}\right)^2. \tag{19}$$

Thus, the total potential energy change of a slightly deformed elastic shell is

$$U_{elastic} = 4\pi r_0^2 T \frac{Y}{8}\frac{\Delta b^2}{r_0^2} = \frac{\pi Y T}{2}\Delta b^2, \tag{20}$$

where T is the thickness of the shell, and the elastic restoration force for a shell is given by

$$F_{shell} = -\frac{\partial U_{elastic}}{\partial \Delta b} = -\pi Y T \Delta b. \tag{21}$$

Not surprisingly, the restoring force is proportional to Δb, and opposite in sign. Comparing to eq. (5) one sees that, as long as the deformation is small and the volume is conserved, only the pre-factor is different between the restoring force of an elastic shell, and the restoring force of a droplet dominated by surface tension. In an equilibrium situation the forces acting on the deformed shell obey

$$0 = F_{opt} + F_{shell}. \tag{22}$$

This can be rearranged to find the elasticity of an elastic shell, which equals Young's modulus times the shell thickness, through the equation

$$YT = -\frac{n_g\langle|Q|\rangle}{2\pi c}\frac{P_{shell}}{\Delta a}, \tag{23}$$

with definitions given above, except that n_g and n_l are now the indices of refraction of the outside, and inside of the cell, respectively. One potential problem is that one cannot distinguish between contributions from surface tension and shell elasticity. However, most objects are dominated either by surface tension (as a viscous droplet), or by shell elasticity (as a vesicle or a cell), hence, in practise it is not problematic. Equation (23) can be rearranged to give

$$P_{shell} = \frac{YT2\pi c}{n_g\langle|Q|\rangle}(-\Delta a), \tag{24}$$

thus pinpionting the linear relationship between laser power and radius deformation.

Deformed object dominated by bulk elasticity. If the deformed object has an elastic restoration force arising from the deformation of the bulk, then this contribution needs to be included in the analysis. This would, *e.g.*, be the case for a eucaryotic cell with a polymerized cytoskeleton. Let the radius of the cell be r_0, Young's modulus of the bulk E, and Poisson's ratio $\nu = 0.5$ (that of an incompressible medium), then the elastic restoration force of the bulk as function of deformation is given by the Hertzian response theory [16]:

$$F_{bulk} = -\frac{4\sqrt{2}}{9} r_0^{1/2} E(\Delta b)^{3/2}. \tag{25}$$

For an equilibrium situation involving a object dominated by its bulk elasticity

$$0 = F_{opt} + F_{bulk}. \tag{26}$$

Hence, the laser power corresponding to a given deformation can be found using eqs. (10) and (25):

$$P_{bulk} = \frac{2^4 c}{9 n_g\langle|Q|\rangle} r_0^{1/2} E(-\Delta a)^{3/2}. \tag{27}$$

Hence, for an object to deform $-\Delta a$ (which is a positive distance), the part of the laser field whose optical momentum is balanced by the elastic force resulting form the deformation of the bulk must have a laser power of P_{bulk}. The relation between P_{bulk} and $-\Delta a$ is not linear, hence, it differs in nature from eqs. (12) and (24).

Deformed object dominated both by shell and bulk elasticity. In the complex case where both surface and bulk elasticities are significant, an equilibrium situation requires

$$0 = F_{opt} + F_{shell} + F_{bulk}. \tag{28}$$

Inserting eqs. (10), (23), and (25), one obtains the total laser power needed to deform both the shell and the bulk by a distance $-\Delta a$:

$$P_{total} = \frac{2^4 c}{9 n_g\langle|Q|\rangle} r_0^{1/2} E(-\Delta a)^{3/2} + \frac{YT2\pi c}{n_g\langle|Q|\rangle}(-\Delta a). \tag{29}$$

Hence, the bulk and surface elasticities of a cell can be found by measuring corresponding values of laser power P_{total} and deformation $-\Delta a$, and fitting an expression of the form $P_{total} = \alpha(-\Delta a)^{3/2} + \beta(-\Delta a)$ and extracting the elasticities from the fitting constants using eq. (29).

Results and discussion. – To compare the prediction with experiments, a 0.1% volume fraction mixture of liquid in gas phase was made and placed in a chamber in the optical tweezers microscope. Simply focusing the trap with laser powers on the order of 200 mW or higher in the sample resulted in the formation and slow steady growth of a drop of the liquid phase. This is because individual colloids, or possibly liquid-phase droplets too small to be seen in the microscope, are attracted to the focus of the laser and condense into a larger drop. By trapping and fusion of drops of different sizes, or by keeping the laser power high for some time interval, visible microscopic drops of different sizes could be created. By moving a large trapped droplet and hence exerting a viscous drag on it, small drops could also be fissioned off from the original droplet, an example of this is shown in the supplementary video. An abrupt increase in laser power resulted in a clearly visible decrease in the radius of the trapped droplet. An example of the laser induced deformation of a droplet at four increasingly higher laser

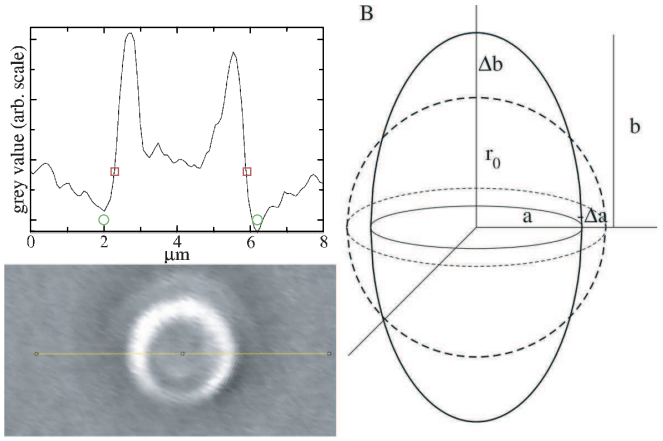

Fig. 3: (A) The graph shows the intensity distribution along the line across the image of the bead. The red squares and green circles exemplify two different ways of defining the drop diameter. (B) A schematic drawing of the non-deformed (dashed line) and deformed drop (solid line). The deformed drop corresponds to a spheroid deformed at 200 mW. The laser direction is upwards.

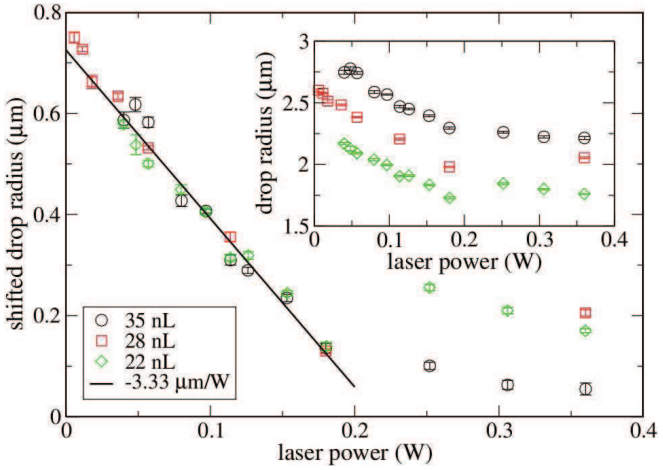

Fig. 4: Normalized droplet radius as a function of laser power for droplets of varying initial size. Full line shows the analytical result. Error bars represent the standard deviation. The inset shows the same results but without normalizing the droplet radius.

powers is shown in fig. 1, where the white ring, as detailed later, approximately corresponds to the diameter of the trapped droplet. If one instead traps a droplet which is not easily deformable by a normal optical trap, as, *e.g.*, a polystyrene bead, then an increase of the laser power will result in an increased scattering force, which will tend to displace the object further away from the laser focus in the direction of the propagating laser. Such a displacement results in an increase of the white ring in the image [17,18]. As we increased the laser power in the present experiment, a similar effect certainly was present, which would tend to increase the diameter of the white ring, but despite this fact we inevitably saw a significant decrease of the white rings diameter with laser power.

A series of measurements where the laser power was increased was always followed by a control measurement of the droplet size at the first laser power. This was done in order to ensure that additional material had not fused to the droplet during the experiment. The time scale of detectable droplet enlargement due to fusion was significantly longer than the run of an experiment and we never detected any volume change between the beginning and end of an experiment.

In order to quantify the deformation of the droplet, the intensity profile along a line across the drop was measured, and the drop diameter taken as the distance between the two minima of the profile, this is shown in fig. 3, where the green circles denote the positions of the intensity minima. The droplet diameter could also be quantified by other measures, *e.g.*, we also defined the diameter as the distance between the two points nearest the center of the drop where the intensity equals the intensity value of the gas phase (shown by red squares in fig. 3).

The result of employing these two different definitions was very similar, the two methods differed only by a constant shift of the radius versus power curves, so the resulting slope of the drop size with laser power was independent of measurement method. This is very important, since our analytical model (eq. (12)) exactly predicts this slope, which is expected not to depend on the absolute size of the drop.

For each trapped drop, the drop diameter was determined eight times at each laser power. The average drop radius normalized with the initial droplet radius as a function of laser power at the sample is shown in fig. 4 for droplets of varying initial size. The data nicely collapses on a common curve at moderate laser powers (below 0.25 W at the sample) showing a clear decrease of droplet size with laser power. The full line in fig. 4 is the theoretical relation given in eq. (12)). The inset shows the data without normalizing by initial droplet radius. At laser powers above 0.25 W the droplet diameter ceases to decrease with laser power.

The change in radius between 0 and 0.25 W is more than half a micron, corresponding to about 20% of the drop size at 0 W, which due to volume conservation and assuming an ellipsoidal shape, requires the length of the drop has increased by more than 50%.

The experimentally observed linear decrease of droplet radius with laser power is in perfect agreement with the analytical model, eq. (12), predicting a slope of $-3.33\,\mu$m/N. The only assumption in the model is that the drop is essentially flat in the region where the light field is significant. In an optical tweezers setup the waist (the full width at half maximum) of the light field is typically less than $1\,\mu$m, and we demonstrated that drops with a radius as small as $2.3\,\mu$m are still well described by the model. At higher laser powers the radius stops decreasing. This is probably because the droplet begins to take a dumbbell (rather than ellipsoidal) shape in order to fill as much of the strongly illuminated region as possible. If the object is a droplet, then its image on a CCD image, focused at its maximum diameter, gives rather precise

information about the true diameter. However, since the focusing volume has an axial extension of approximately $0.5\,\mu$m, a CCD image of a dumbbell focused on the waist would not clearly image the smallest waist, but rather give information on the largest diameter within the focal region. Hence, even if the waist of a dumbbell shaped droplet continues to decrease, we would not be able to image it, but rather see the largest diameter within the focal region.

Conclusion. – We have demonstrated that drops trapped by electromagnetic radiation also become deformed by the electromagnetic field. The deformation increases with laser power up to a certain threshold and can be as large as 20% in diameter and 50% in length. For low surface tension drops even at moderate laser powers (50 mW at the sample) the deformation is significant and easily detectable. The rate of deformation with respect to laser power is constant and very well described by a simple analytical model. This model can be used to explore physical constants of soft materials, *e.g.*, it is straight forward to determine the drop surface tension, knowing the indices of refraction and the laser power. The simplicity of a drop with only surface tension as a restoring force makes such a system desirable to use for calibration of, *e.g.*, optical stretcher assays. In addition, we provided analytical tools to treat the case of optically stretched objects whose deformation is dominated by an elastic shell deformation, as, *e.g.*, a vesicle or a cell without a polymerized cytoskeleton, or dominated by an elastic bulk deformtion, as, *e.g.*, a cell with a relatively stiff cytoskeleton, or a combination of both these contributions. These three cases constitute the biologically most relevant situations, and future investigations will include applying these methods to living cells.

* * *

We thank F. Czerwinski for help with the optical tweezers setup, and acknowledge financial support from the University of Copenhagen Excellence program.

REFERENCES

[1] Ashkin A., Dziedzic J. M., Bjorkholm J. E. and Chu S., *Opt. Lett.*, **11** (1986) 288.
[2] Svoboda K. and Block S. M., *Opt. Lett.*, **19** (1994) 930.
[3] Hansen P. M., Bhatia V. K., Harrit N. and Oddershede L., *Nano Lett.*, **5** (2005) 1937.
[4] Guydosh N. R. and Block S. M., *Nature*, **461** (2009) 125.
[5] Guck J., Ananthakrishnan R., Mahmood H., Moon T. J., Cunningham C. C. and Kas J., *Biophys. J.*, **81** (2001) 767.
[6] Dharmadhikari J. A., Roy S., Dharmadhikari A. K., Sharma S. and Mathur D., *Opt. Express*, **12** (2004) 1179.
[7] Bambardekar K., Dharmadhikari A. K., Dharmadhikari J. A., Mathur D. and Sharma S., *J. Biomed. Opt.*, **13** (2008) 064021.
[8] Suresh S., Spatz J., Mills J. P., Micoulet A., Dao M., Lim C. T., Beil M. and Seufferlein T., *Acta Biomater.*, **1** (2004) 15.
[9] Ward A. D., Berry M. G., Mellor C. D. and Bain C. D., *Chem. Commun.*, **43** (2006) 4515.
[10] Fortuna S., Colard C. A. L., Troisi A. and Bon S. A. F., *Langmuir*, **25** (2009) 12399.
[11] Lekkerkerker H. N. W., Poon W. C. K., Pusey P. N., Stroobants A. and Warren P. B., *Europhys. Lett.*, **20** (1992) 559.
[12] de Gennes P.-G., Brochard-Wyart F. and Quéré D., *Capillarity and Wetting Phenomena* (Springer) 2003.
[13] Casner A. and Delville J.-P., *Phys. Rev. Lett.*, **87** (2001) 054503.
[14] Casner A. and Delville J.-P., *Phys. Rev. Lett.*, **90** (2003) 144503.
[15] Griffiths D. J., *Electrodynamics* (Prentice Hall) 1999.
[16] Timoshenko S., *Theory of Elastic Stability* (McGraw Hill) 1982.
[17] Crocker J. C. and Grier D. G., *J. Colloid Interface Sci.*, **179** (1996) 298.
[18] Hansen P. M., Dreyer J. K., Ferkinghoff-Borg J. and Oddershede L., *J. Colloid Interface Sci.*, **287** (2005) 561.